Optical Wireless for Intravehicle Communications: Incorporating Passenger Presence Scenarios

Matthew D. Higgins, *Member, IEEE,* Roger J. Green, *Senior Member, IEEE,*
and Mark S. Leeson, *Senior Member, IEEE*

***Abstract*—Through the implementation of a simple, linearly scalable $1\,\mathrm{W}$ IR transmitter, located centrally on the ceiling of a sports utility vehicle, and for 15 passenger configurations, an analysis into the received power, power deviation, minimum bandwidth and maximum RMS delay spread is provided for the regions of the vehicle most likely to benefit from the deployment of intra-vehicle optical wireless communication systems. Several specific regions, including the areas around a passengers legs, arms, necks and shoulders are shown to have beneficial channel characteristics for the use of personal electronics equipment such as laptops, tablet PCs or wireless headphones. Similarly, a region around the headrest of the front seat is shown to have potential for the deployment of an in car entertainment solutions independent of the passenger configuration. This analysis, the first to introduce the concept of channel variation from multiple passenger configurations, aims to show that optical wireless is a potential candidate for future intra-vehicular communication systems.**

***Index Terms*—Optical Wireless, Wireless LAN, VANET, Channel Model.**

I. Introduction

CURRENT mass production vehicles contain an ever growing plethora of interconnected electronics devices. These devices range from the functionally integral sub-systems such a fly-by-wire technologies, engine management or safety actuators, to consumer focused sub-systems such as navigation and audio visual (AV) entertainment solutions [1], [2]. Further to this, vehicle passengers are also bringing third party personal electronic equipment such as mobile phones, tablet PCs or handheld games consoles into the cabin. This increase and subsequent dependency on electronics in or around vehicles, increases the cost and complexity of their design and manufacturing, not to mention, potential reductions in reliability and fuel efficiency due to the increased use of wiring harnesses.

One possible way of mitigating these effects of increased vehicular electronics is to adopt wireless communications where possible. An interesting and emerging [3] branch of available wireless communications techniques is Optical Wireless (OW), which combines the mobility of radio frequency (RF) wireless communications with the high bandwidth availability of fixed optical communications. In a recent review paper [4], it was shown that OW may provide a compatible solution to the concept of intra-vehicular communications, defined to be the process of irradiating the interior (or section) or the vehicle with infrared (IR) radiation to serve as the communication link between anything from simple user-vehicle interface devices such as window or air conditioning controllers, to more advanced devices associated with AV entertainment units or computer consoles.

This initial review was followed by [5] and [6] which provided the first detailed simulations into OW viability. In [5], an empty Sports Utility Vehicle (SUV) was assumed to have a simple single element transmitter placed upon the ceiling in tandem with receivers with a FOV $= 65°$. It was shown that, based upon a $1\,\mathrm{W}$ transmitter, received powers of $49\,\mu\mathrm{W\,cm^{-2}}$ could be achieved in the rear seating areas with associated bandwidths $\geq 300\,\mathrm{MHz}$. Further to this, the front seat headrests could receive powers of up to $28\,\mu\mathrm{W\,cm^{-2}}$ but with limited bandwidths of $56\,\mathrm{MHz}$. Based upon the same scenario, the work of [5] was expanded in [6] but with a reduced receiver FOV $= 45°$ as well as taking into consideration the RMS delay spread of the channel. A reduced FOV was chosen to begin investigating a more 'directional' system that might increase the bandwidth of the rear passenger seats in selected areas with the known compromise of reducing the total received power. Peak power in the rear seats only reduced slightly to $46\,\mu\mathrm{W\,cm^{-2}}$ and increased directionality was shown with higher bandwidths in the regions of the passengers head rests and door frames as predicted. It can be noted, the need for directionality (or not) is still under consideration as it is well known that a wider FOV, whilst allowing for increased flexibility in alignment, reduces bandwidth and increases ambient light noise collection.

For all of the results presented in [5] and [6], which attempted to narrow down where and how-well an OW system will perform when deployed within a vehicle, the work presented however, did not consider the presence of either the driver or passengers. In this paper, the original work is substantially extended though the analysis of channel performance metrics over 15 different scenarios. Based upon this extended deployment scenario analysis, it is hoped that a system designer or industrial expert associated with the vehicular industry will have further confidence in investing resources towards future OW communications technology as an alternative to RF solutions.

The remainder of this paper is ordered as follows. Section II details the SUV and passenger deployment scenarios, theory of

The authors are with the School of Engineering, University of Warwick, Coventry, CV4 7AL, UK.
E-mail: {m.higgins;roger.green;mark.leeson;}@warwick.ac.uk

Manuscript version: 12th May 2013

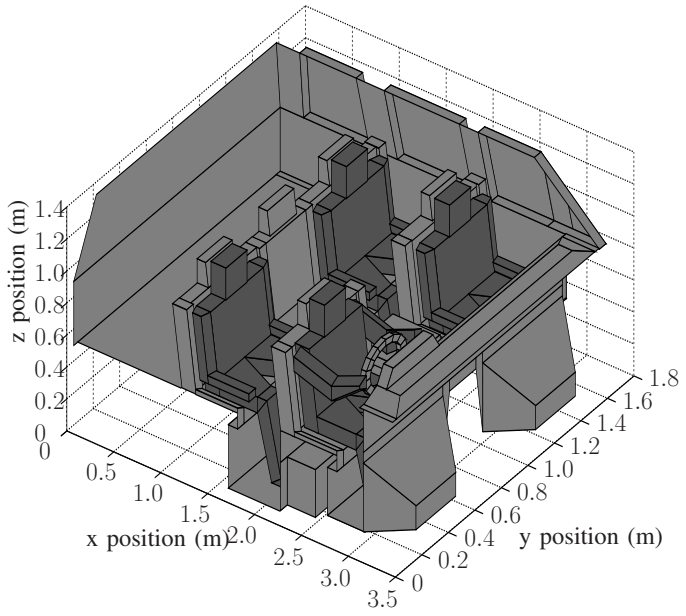

Fig. 1. SUV structure for the which the OW system is deployed within. The specific scenario shown is the case of the driver and three 'arms down' passengers being present.

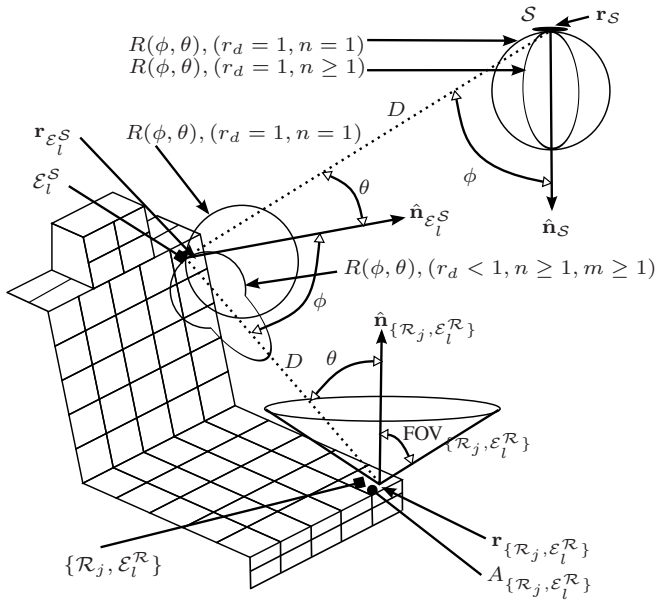

Fig. 2. Source, receiver and reflector geometry.

IR propagation and reflection and the calculations required to determine the impulse response between a source and receiver. Section III provides the simulation results of the OW channel and how it impacts future system performance. Section IV then clarifies where the next stage in the research should be directed, followed by concluding remarks in Section V.

II. System Model

A. Vehicle Environment

The cross sectional representation of the internal structure of the SUV at maximum capacity is shown in Fig. 1. The internal structure, comprising floor, ceiling, fascias, seats, steering wheel etc. is generated from the arrangement of 296 planar polygons, whilst each passenger is formed by the arrangement of a further 66 planar polygons. The system environment has been made as realistic as is practically possible and includes features such as angled foot wells, recessed windows and bevelled edge seats. Furthermore compared to the model used in [5] and [6], extra 'blind spots' in the form of gaps between seats and around the car doors have been added to improve its realism.

In this paper, multiple scenarios are considered. Firstly it is assumed that the interior structure does not change and that the driver is always present and has their arms up towards the steering wheel as shown in Fig. 1. Then, 7 further scenarios are considered with every combination of the other 3 passengers being either present or absent with their arms up (like the driver), and a further 7 scenarios with every combination of the other 3 passengers being either present or absent with their arms down (as in Fig. 1). Ergo, a total of 15 scenarios is considered and later analysed. For further reference, Fig. 1 is one of the two most complex scenarios (the other being when all three passengers are present with their arms up) and consists of a total of 560 planar polygons. Based upon the feedback from presenting of [5], the model has had its width increased by 20 cm and height reduced by 10 cm to take account of a possible industrial focus change in vehicle design to the more compact SUVs.

Each different material found within the vehicle, including those that make up the passengers e.g skin, is assumed to abide by a Phong [7] reflection model for which, the emitted or reflected radiation intensity profile, $R(\phi,\theta)$, is given by [8], [9]:

$$R(\phi,\theta) = P_{\mathcal{S}}\left[\frac{r_d(n+1)\cos^n(\phi)}{2\pi}+\ldots \frac{(1-r_d)(m+1)\cos^m(\phi-\theta)}{2\pi}\right] \quad (1)$$

Where $\phi\in[0,\pi/2]$ and $\theta\in[0,\pi/2]$ are the angles of observation and incidence relative the surface normals respectively, $r_d\in[0,1]$ represents the ratio of incident signal reflected diffusely, m is the order of the specular component, n is the order of the diffuse component and $P_{\mathcal{S}}$ is the power of the radiation to be emitted. The use of the more advanced Phong reflection model is necessary due to the abundance of glass in this application, commonly known to be a specular reflector, and so cannot be modelled using the traditional assumptions of Lambertian reflectors within the system deployment environment [10], [11].

Referring to Fig. 2, the geometries with example generalised radiation profiles are shown for cases when the reflection profile is either Phong ($r_d<1,n\geq 1,m\geq 1$), high order Lambertian ($r_d=1,n>1$) or traditional pure Lambertian ($r_d=1,n=1$). In order to determine accurate values for m,n and r_d in (1), along with the reflectivity $\Gamma\in[0,1]$ of several common vehicle interior materials, the open access

TABLE I
REFLECTION PROPERTIES USED DURING SIMULATION

Material	Γ	r_d	m	n
Glass	0.03	0	280	1.0
Fabric (Ceiling)	0.50	1.0	1.0	1.0
Fabric (Seats/Trousers)	0.40	1.0	1.0	1.0
Fabric (Floors/Boot space)	0.30	1.0	1.0	1.0
Shoe Leather	0.30	1.0	1.0	1.0
Fabric (Torso Shirt)	0.30	1.0	1.0	1.0
Fascia Plastic	0.60	1.0	1.0	1.0
Skin/Hair	0.45	1.0	1.0	1.0

Columbia-Utrecht Reflectance and Texture (CUReT) database [12] was employed.

From the databases 61 available materials, 'Sample 4 - Rough Plastic' is the most similar to typical fascia plastic used on car door interiors, window sills and dashboards. Through a Oren-Nayer fitting process [13], it was found that the material exhibited a 0.6 reflectivity with 96% of it being diffuse. 'Samples 7,18,19,42,44 and 46', which represent the materials of Velvet, Thick Rug, Fine Rug, Corduroy, Linnen and Cotton respectively, are ideal candidates for representing the vehicles interior upholsteries and passenger cloths. Via the same Oren-Nayer fitting process, the upholsteries reflectivity ranged between 0.12 and 0.57 for which the heavier samples, such as those used on the car floor, having a lower reflectivity, and the finer materials, such as the thin fabric found on a car ceiling, having a higher reflectivity. Of these reflectivity values, the percentage of power contained within the diffuse component ranged between 94% and 99%. Therefore, based upon their measurements, and to reduce the simulation complexity (via the simplification of (1)), each of the fabrics and the fascia plastic will be assumed to be fully diffuse $r_d = 1$, with our interpretation of the their respective reflectivities shown in Table I. The databases 'Sample 39 - Human Skin' provdes a reflectivity of approximatly 0.45 under the same fully diffuse assumptions made for the fabrics. Finally, for the reflectivity properties of the glass, the required parameters were derived from the measured results in [8] with the resulting approximation that the glass is fully specular, with a high directivity and low reflectivity. It should be noted that each of these values is in itself an approximation for the purpose of this work. The values provide in CUReT are not strictly for IR frequencies but they do enter the red spectrum with enough detail as to make sensible assumptions.

B. Source, Receiver and Reflector Model

The transmission source, $\mathcal{S}$, in this scenario is considered to be an IR LED located centrally upon the ceiling with position vector $\mathbf{r}_{\mathcal{S}} = [1.7, 0.82, 1.38]$, orientated vertically downwards with unit length orientation vector $\hat{\mathbf{n}}_{\mathcal{S}}$. The radiation emission profile, $R(\phi, \theta)$, with power $P_{\mathcal{S}}$, is assumed to be uniaxial symmetric, with respect to $\hat{\mathbf{n}}_{\mathcal{S}}$, and ideal Lambertian as given by (1) setting $n = 1$ and $r_d = 1$.

In order to determine the suitability of the OW channel for communication purposes, and to determine where in the vehicle high levels of IR radiation with suitable bandwidth characteristics are located, it is necessary to model the existence of J single element receivers R_j. It is assumed that each receiver is of the same specification such that $\mathcal{R}_j = \mathcal{R}_{j+1}$, and this allows for the results in Section III to describe both a system with J receivers at multiple locations or one receiver at J locations without any loss of generality.

To determine the position and orientation of each of the J receivers (or J locations), each of the planar polygons that make up the deployment environment is bilinearly interpolated [14] at a resolution of 10 segments per meter (100 segments per square meter). This interpolation then provides the resultant location vector $\mathbf{r}_{\mathcal{R}_j}$, unit length orientation vector $\hat{\mathbf{n}}_{\mathcal{R}_j}$ identical the respective surface normal of the original polygon, an active optical collection area $A_{\mathcal{R}_j} = 1\,\text{cm}^2$, and field of view $\text{FOV}_{\mathcal{R}_j} = 45°$, defined as the maximum uniaxial symmetric incident angle of radiation with respect to $\hat{\mathbf{n}}_{\mathcal{R}_j}$, that will generate a current within the photodiode. This process is repeated for every planar polygon within the scenario and for every scenario, meaning that for the simplest scenario, i.e. only the driver is present $J = 3269$, whilst for the two most complex scenarios, i.e.the driver and three further passengers present with either their arms up or down $J = 4023$. The decision to set $A_{\mathcal{R}_j} = 1\,\text{cm}^2$ is based upon a desire to keep the forthcoming results as generalised as possible, allowing for the comparison of the system performance presented here to be directly comparable to papers such as [15]. Moreover, due the linearity of the channel, in the event using smaller $A_{\mathcal{R}_j}$ values, the received power values should simply be scaled appropriately.

Given the definitions and material properties of the vehicle's internal structure provided in Section II-A, each of the planar polygons is bilinearly interpolated into L elements $\mathcal{E}_l$ at a resolution of ΔA_k, the desired number of elements per meter. Based upon the interpolation, the resultant elements $\mathcal{E}_l$ will have an associated area $A_{\mathcal{E}_l} = 1/\Delta A_k^2$, unit length orientation vector $\hat{\mathbf{n}}_{\mathcal{E}_l}$ determined from the normal vector of the original non-interpolated plane at a position vector $\mathbf{r}_{\mathcal{E}_l}$. The element will then behave as a receiver, $\mathcal{E}_l^{\mathcal{R}}$ with a hemispherical FOV for which the incident power $P_{\mathcal{E}_l^{\mathcal{R}}}$ can be determined, before acting as a source $\mathcal{E}_l^{\mathcal{R}}$, with a radiation emission profile $R(\phi, \theta)$, as given by (1) setting the parameters to the respective properties of the element in Table I and with $P_{\mathcal{S}} = \Gamma P_{\mathcal{E}_l^{\mathcal{R}}}$.

C. Impulse Response Calculations

The IR radiation incident upon a receiver $\mathcal{R}_j$ will be the result of radiation emitted from the source $\mathcal{S}$ that has propagated directly through an unobstructed LOS path, and/or from the radiation that has undergone a finite number k, reflections off the internal surfaces of the vehicle. It has previously been shown [15], [16] that for an intensity modulation, direct detection (IM/DD) channel, where the movement of the transmitter, receiver or reflectors within the environment are slow compared to the bit rate of the system, no multipath fading occurs, and, as such, can be modelled as a LTI channel with impulse response $h(t; \mathcal{S}, \mathcal{R}_j)$ given by [15]:

$$h(t; \mathcal{S}, \mathcal{R}_j) = \sum_{k=0}^{k} h^k(t; \mathcal{S}, \mathcal{R}_j) \tag{2}$$

where $h^k(t, \mathcal{S}, \mathcal{R}_j)$ is the impulse response of the system for the radiation undergoing k reflections between $\mathcal{S}$ and $\mathcal{R}_j$.

Assuming that the source $\mathcal{S}$ emits a unit impulse at $t = 0$, i.e. setting $P_{\mathcal{S}} = 1\,\text{W}$, then the LOS $(k = 0)$ impulse response is given by the scaled and delayed Dirac delta function, i.e.,

$$h^0(t; \mathcal{S}, \mathcal{R}_j) \approx R(\phi, \theta) \frac{\cos(\theta) A_{\mathcal{R}_j}}{D^2} V\left(\frac{\theta}{\text{FOV}_{\mathcal{R}_j}}\right) \delta\left(t - \frac{D}{c}\right) \tag{3}$$

where, with reference to Fig. 2, $D = ||\mathbf{r}_{\mathcal{S}} - \mathbf{r}_{\mathcal{R}_j}||$ is the distance between the source and receiver, c is the speed of light, ϕ and θ are the angles between $\hat{\mathbf{n}}_{\mathcal{S}}$ and $(\mathbf{r}_{\mathcal{R}_j} - \mathbf{r}_{\mathcal{S}})$ and between $\hat{\mathbf{n}}_{\mathcal{R}_j}$ and $(\mathbf{r}_{\mathcal{S}} - \mathbf{r}_{\mathcal{R}_j})$ respectively. $V(x)$ represents the visibility function, where $V(x) = 1$ for $|x| \leq 1$ and $V(x) = 0$ otherwise.

For radiation undergoing $k > 0$ reflections, the impulse response is given by:

$$h^k(t; \mathcal{S}, \mathcal{R}_j) = \sum_{l=1}^{L} h^{(k-1)}(t; \mathcal{S}, \mathcal{E}_l^{\mathcal{R}}) * h^0(t; \mathcal{E}_l^{\mathcal{S}}, \mathcal{R}_j) \tag{4}$$

Where $*$ denotes convolution, and the $(k-1)$ impulse response $h^{(k-1)}(t; \mathcal{S}, \mathcal{E}_l^{\mathcal{R}})$ can be found iteratively from [17]:

$$h^k(t; \mathcal{S}, \mathcal{E}_l^{\mathcal{R}}) = \sum_{l=1}^{L} h^{(k-1)}(t; \mathcal{S}, \mathcal{E}_l^{\mathcal{R}}) * h^0(t; \mathcal{E}_l^{\mathcal{S}}, \mathcal{E}_l^{\mathcal{R}}) \tag{5}$$

where all the zero order $(k = 0)$, responses in (4) and (5) are found by careful substitution of the variables in (3).

III. Results

A ray-tracing package, with a specific emphasis on efficient bilinear surface interpolation [18] and intersection sub-routines [19], was developed in MATLAB to determine the source to receiver impulse response as detailed in equations (1) through (5). One known issue of equation (5) is that the time to calculate the solution is proportional to k^2 [17], such that for all the results presented here, k is limited to 3, and for each order, the segmentation of the bilinear interpolation is set to $\Delta A_1 = 25$, $\Delta A_2 = 6$ and $\Delta A_3 = 2$. Please note, these ΔA_k values are for the segmentation of the surfaces forming the reflecting (and sequentially transmitting) elements, not the receivers which as stated earlier, are generated from a bilinear interpolation with a resolution of 100 segments per square meter independent of the impulse response order. It is also possible for the reader to increase (or decrease) the value of both k and any of the ΔA_k values as they see fit should a higher (or lower) fidelity be required. We do however want to stress that the choice of values will highly dictate the computational time required, where for this work, the compromise was made through experience that the results are within a scenario dependent 10% of including a higher order at the cost of $\sim 72\,\text{h}$ simulation time on a modern machine. For further clarification of this issue, the reader is directed to [17] and [20] for some emperical discussions. It can also be observed that the resultant impulse response in (2) is a finite sum of scaled delta functions which for the results presented are smoothed by sub-dividing the time into bins of width $\Delta t = 0.1\,\text{ns}$ prior to summation [15].

Compared to earlier work in [6], where only 1 scenario was investigated, it is now necessary to adjust the way in which the results are presented. Here, a total of 15 scenarios have been explored, and as such, displaying a continuous set of figures is not only inefficient, but difficult to interpret. Therefore, in this paper, four quantities are to be shown:-

- Received power baseline: Here the total power received, as defined by $H(0; \mathcal{S}, \mathcal{R}_j) = \int_{-\infty}^{\infty} h(t; \mathcal{S}, \mathcal{R}_j) dt$, is shown for the scenario where only the driver is present within the vehicle. These values therefore provide the baseline for which passenger presence can be measured against. The values will be provided as absolute values in μW as this allows for easy comparison with the results of most the notable works by Barry [15]. Given also, that as mentioned, the results are also presented as being normalised from a 1 W source, if the reader wishes to know the path loss in dB only a simple calculation needs to be performed.
- Received power change: Here, the received power for the remaining 14 cases is analysed and the greatest absolute change of a non-zero received power is compared against the baseline and recorded. The requirement for non-zero quantities is necessary as for example, the presence of a passenger on the seat will block specific receivers. These receivers should therefore be excluded from the power change as they cannot be used in practice if a passenger is present at that location. Therefore, for a given receiver location, one can take the baseline value and with the addition or subtraction of the change value at that same location, one can infer the maximum dynamic range of received powers for any combination of passengers where the receiver is still valid, i.e not directly blocked. The authors acknowledge here that representation of the results is actually quite hard for the difference results. As such, here, the values are in dB as this is most commonly requested by readers interested in change from the baseline.
- Minimum channel bandwidth: Here, due to the application of plotting the quantity $H(0; \mathcal{S}, \mathcal{R}_j)$, where all temporal information is lost, the minimum non-zero bandwidth, found via the DTFT of $h(t, \mathcal{S}, \mathcal{R}_j)$, of all 15 scenarios is shown. In showing this quantity as supposed to a change quantity, the results provide a system designer with a bandwidth value that can be guaranteed at a given location independent of the passengers presence provided they are not blocking the receiver.
- Maximum RMS delay spread: Here, the maximum non-zero RMS delay spread Λ, as given by [21]:

$$\Lambda = \sqrt{\frac{\int_{-\infty}^{\infty} (t - \Upsilon)^2 h^2(t; \mathcal{S}, \mathcal{R}_j) dt}{\int_{-\infty}^{\infty} h^2(t; \mathcal{S}, \mathcal{R}_j) dt}} \tag{6}$$

where Υ is defined as:

$$\Upsilon = \frac{\int_{-\infty}^{\infty} t h^2(t; \mathcal{S}, \mathcal{R}_j) dt}{\int_{-\infty}^{\infty} h^2(t; \mathcal{S}, \mathcal{R}_j) dt} \tag{7}$$

for each of the 15 scenarios is shown. The maximum value is provided as this is worst case option for a system

designer and as such this quantity provides the maximum RMS delay spread possible at any location independent of passenger presence provided the receiver is not blocked.

These four quantities are shown in Figures 3 through 6 where, one may see that unlike Figure 1 where the passengers have been illustrated, in the results, only the driver is shown as the driver is the only consistent passenger in the vehicle. In the other 14 scenarios analysed, passengers are considered either absent or present with either their arms up or down, and so they are not consistent and so impossible to illustrate graphically. In other words, provided the receiver is not blocked by a passenger being present, it is considered within the analysis. For example, if one wanted to know the effects of only the driver and one further passenger situated in the rear seat (also driver side) being present, one could make a perfectly valid inference of the results by simply discounting the specific receiver locations that will be blocked.

A. Rear Passenger Seats

Consider first the rear passenger seat results as shown in Figures 3 and 4. Directly under the source, a maximum received baseline power (Fig. 3(a)) of 45 µW is located centrally on the middle seat which reduces to 15 µW at the seat corner edges. This area is ideal for the passengers portable devices such as laptops, tablet PC's or hand held games consoles. Incorporating the possible passenger scenarios, Fig. 3(b) shows that in the central region, the received power deviates by no more than 0.1 dB compared to the baseline. This is a promising result for the viability of OW in this application considering up to 3 more people are present. In the gaps between the passengers legs, there can be a dramatic drop in power of up to 10 dB. This is an obvious property of OW and the source transmitter geometry needs further careful thought. These power levels have an associated minimum bandwidth (Fig. 4(a)) of 29 MHz increasing to over 100 MHz with a sub nano-second RMS delay spread (Fig. 4(b)). Provided the received power dynamic range can be accounted for in the receiver design, this level of bandwidth availability should be sufficient for in car communications requirements.

A further area of potential OW device deployment shown in previous work [6] was the area around the head and shoulders of the rear passengers, as it would be conceivable they may wish to use IR headphones or hands free voice equipment. The baseline values (Fig. 3(a)) range from between 17 µW and 40 µW which when one considers the passenger scenarios (Fig. 3(b)) fall by a maximum of 0.2 dB. The minimum available bandwidth (Fig 4(a)) available over the area is 82 MHz with a virtually negligible (sub-pico second) RMS delay spread as shown in Fig. 4(b). All of these quantities are well in excess of any channel requirements for an OW device of the headphone type.

So far, OW device deployment looks promising. However, successful end-user adoption requires that the technology be user friendly. One such concern is that passengers may either drop or stow portable devices in the foot wells. Under these circumstances it might not be necessary for high speed communications but an ability to be 'polled' by the source

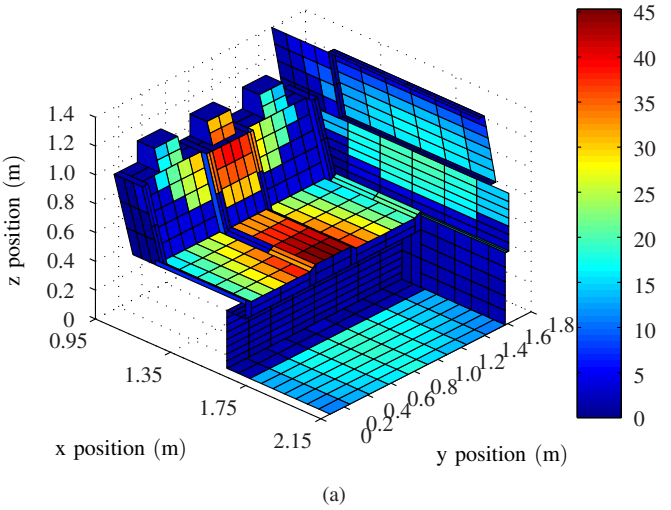

Fig. 3. Rear passenger seat: (a) Baseline values without additional passengers in µW. (b) Power change due to additional passengers in dB.

should remain. As such consider again Fig. 3, where it can be seen that up to 19 µW allowing for a reduction from 0 dB in central locations down to −12 dB near a passengers foot. This power may be enough for simple polling routines, especially given the highly preferential 44 MHz of minimum bandwidth shown in Fig. 4(a). RMS delay spread is mostly in the sub-nano second range although there are instances at the intersection between the floor and the seat edge which is susceptible to slightly higher values approaching 2 ns.

Considering the deployment of fixed user-vehicle OW devices such as window, air-conditioning, heating or AV controllers that could be located within the forward section of the interior car door for example, a baseline received power (Fig. 3(a)) of 18 µW is possible that upon user presence (Fig. 3(b)) is reduced by up to 10 dB. Given that this location has an associated bandwidth in excess of 100 MHz and a sub-pico second RMS delay spread (Fig. 4), there should be little problem using any devices of this nature with the channel available.

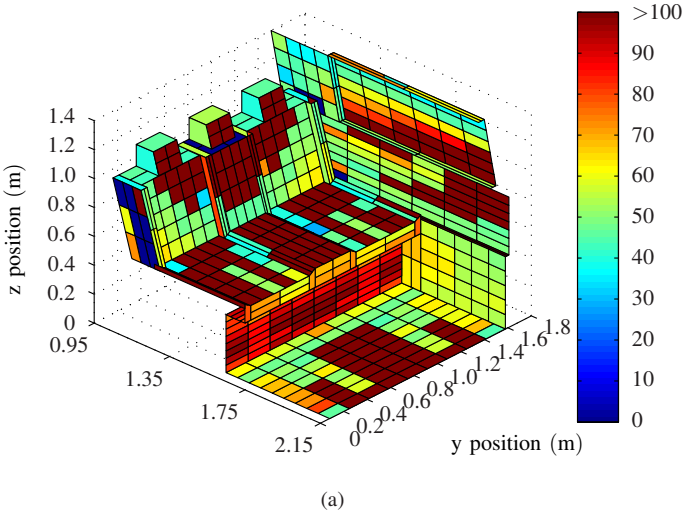

(a)

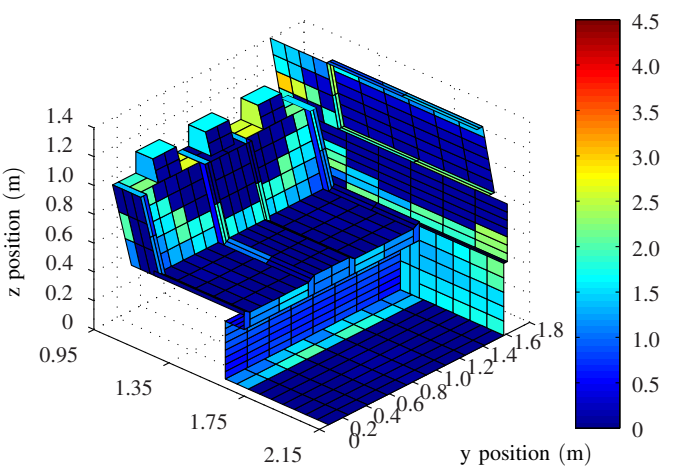

(b)

Fig. 4. Rear Passenger seat values over all scenarios. (a) Minimum received bandwidth (in MHz). (b) Maximum RMS delay spread (in ns).

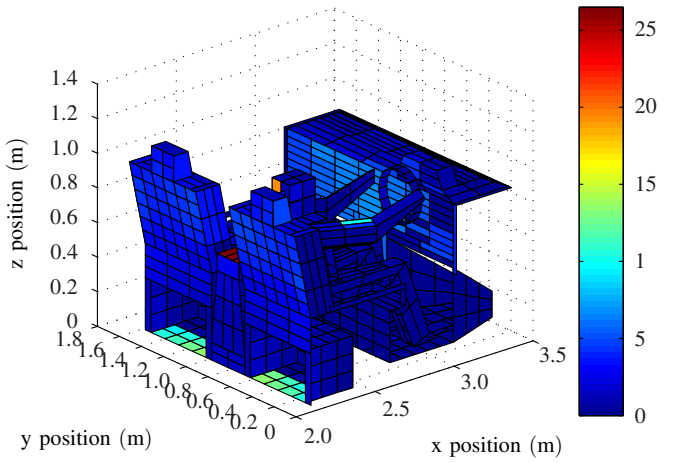

(a)

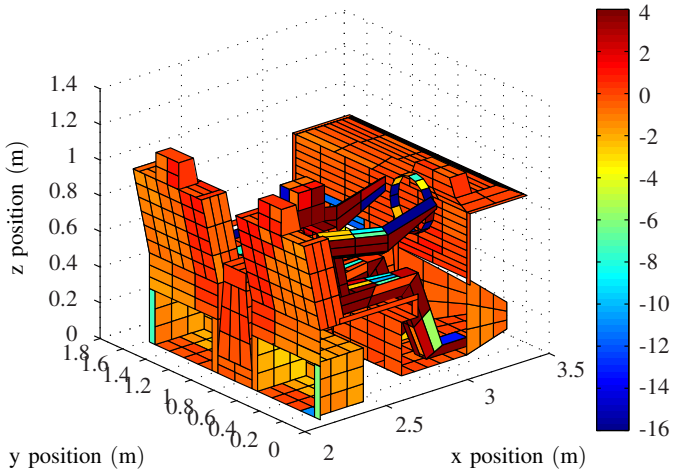

(b)

Fig. 5. 'Forward looking' regions of the SUV: (a) Baseline values without additional passengers in μW. (b) Power change due to additional passengers in dB.

B. Rear Passenger View

One of the growing areas of vehicular electronics investment, is in the deployment of AV entertainment equipment such as TV's DVD players or games consoles. With this in mind, the next area of focus for analysis is the back of the front seat headrests and the arm-rest/storage compartment between the front seats as shown in Figures 5 and 6. In the headrest area (Fig. 5(a)), it can be seen that a baseline power of between $3.8\,\mu$W and $4.2\,\mu$W is received and that this power is reduced by no more than $0.8\,$dB under all passenger scenarios considered (Fig. 5(b)). Furthermore, at these locations (Fig. 6), a bandwidth in excess of $55\,$MHz with a maximum RMS delay spread of $1.95\,$ns can be utilised. Considering these values for a moment, it may be of ones opinion that the received power level is a little low, and so it should also be pointed out that at this stage in the investigation, this result is based upon a non-optimised source-receiver position and/or orientation.

Considering the arm-rest/storage compartment between the front seats shown in Fig. 5, a received baseline power of $26\,\mu$W, that under consideration of the 14 passenger scenarios is reduced by no more than $0.5\,$dB is present with an associated bandwidth in excess of $100\,$MHz with a sub-pico second RMS delay spread. These values are almost certainly ideal for high bandwidth sources or interface devices such as DVD players or games consoles which could all connect via an IR link to the central ceiling base station.

IV. Feasibility and Future Directions

A. Networking and Protocol

A present day 'snapshot' of communication networks within vehicles would show, on one hand, a range of specifically tailored wired technologies, and on the other, a range of fairly generic wireless technologies [22]–[24]. For example, on the wired front, whether electrical or optical, a vehicle designer can adopt any combination of CAN, TTCAN, LIN, TTP, BYTEFLIGHT, FLEXRAY, MOST or IDB-1394 for example with each one deliberately promoting specific advantages for

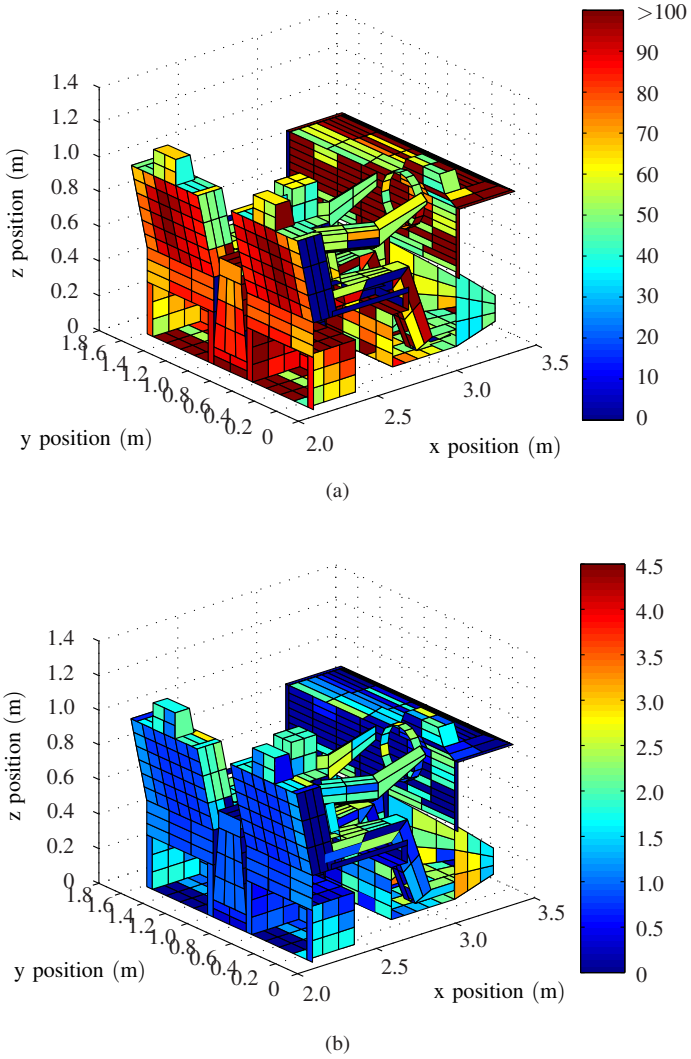

Fig. 6. The 'forward looking' region of the SUVs values over all scenarios. (a) Minimum received bandwidth (in MHz). (b) Maximum RMS delay spread (in ns).

target applications [25]–[30]. On the RF wireless front, a vehicle designer has the option of using standardised technologies such as IEEE 802.11, Bluetooth, UWB or ZigBee for which, based upon the target application, the designer will adopt one based upon which one best fits [31]–[33].

The work presented here based upon OW, is still an open topic, yet to even prove its feasibility. Therefore the scope of the investigation is still limited to understanding the physical layer. The aims here are to know where an OW system can be deployed and what basic hardware requirements would be needed to establish a link of currently unknown performance. Furthermore, although it is known that link reciprocity or bi-directionality will be required in the future, it is not yet considered as the transmitting location (for the uplink) is not yet reasonably established. One of the key logical next steps for the research is to determine by what means a return signal may be instigated. If anything, it is hoped this work presented so far can provide some impetus to portable device manufactures or vehicular equipment OEM's to join the debate here.

B. Optical Noise

All the results presented so far in this paper are for the transmission, propagation and reception of the IR signal. A complete analysis of the noise components has yet to be fully undertaken, partly due to complexity of the deployment application. In the authors' opinion, this vehicular application could be described as a "quasi-indoor-outdoor" crossover. For example, let it be assumed that the system comprises an IR LED transmitter centred at an eye-safe $\lambda = 1330\,\text{nm}$, [34] in conjunction with a generic wide-angle FOV IR receiver with a matched $\Delta\lambda = 66\,\text{nm}$ thin-film optical filter [35, p. 43]. It is also known from Section III that the incident optical signal will peak at $45\,\mu\text{W}\,\text{cm}^{-2}$. In terms of the potential optical noise-generating sources, one can narrow this down to interior lighting, other vehicles' headlights, street lights, and solar radiation from the sun. Most vehicles do not have interior lights due to night time driving requirements, so this can be discounted from our analysis. Most headlights on modern vehicles are based upon high efficiency, Xenon-type bulbs which are designed to be as 'white' as possible with hints of blue, so these can also be discounted. Similarly, street lights in the UK are traditionally Calcium-based, and yellow. This leaves, therefore, only sunlight to contend with on a simplified system, which is indeed very similar to indoor applications, if not slightly simpler, as there is less artificial ambient light, and zero cyclostationary signals present.

This therefore can lead to a simplified argument that, under a bright skylight, where the incident optical power is $5.8\,\mu\text{W}\,\text{cm}^{-2}\,\text{nm}^{-1}$, then for an optical bandwidth of $100\,\text{nm}$, then this equates to an ambient illumination level of $580\,\mu\text{W}\,\text{cm}^{-2}$. This leads to an adverse condition for Optical signal to noise ratio (SNR), according to the following argument: the ambient illumination is $(580/45) = 12.9$ times the optical power density of the wanted signal, resulting in the two effects of firstly the signal being masked by the ambient, and an increase in shot noise by 12.9 times in terms of electrical power at the front end detector stage in the receiver. How is this serious situation to be avoided, then? In fact, it's a matter of optimising the wanted-to-unwanted optical power ratios, by making sure that that the ambient illumination in the wavelength range of particular interest is blocked as much as possible. A coating on the windows of the vehicle would only need to provide just over $11\,\text{dB}$ (or more) of attenuation in the near infrared for reduction of ambient illumination to the same level as the required signal, but $20\,\text{dB}$ would be very easy to obtain and would virtually eliminate the problem all together.

C. Marque and Model

The work presented herein has been based upon a SUV type of vehicle for the reason set out in Section I. An additional reason for the choice was the fact that an SUV can be interpreted as a somewhat 'square' vehicle, a suitable iteration of previous work on indoor optical communications where the impulse response calculations originally existed. Future work

in this area will need to consider a wider range of vehicles and furthermore, a wide range of material compositions for the interiors that go beyond our approximations based upon the CUReT [12] database.

V. Conclusions

Through the use of a simple, linearly scalable $1\,\mathrm{W}$ IR transmitter, located centrally on the ceiling of an SUV type vehicle, and for 15 passenger configurations, the received power, power deviation, minimum bandwidth and maximum RMS delay spread is provided for the regions of the vehicle most likely to benefit from the deployment of intra-vehicle OW communication systems. Specifically, several regions are highlighted as having potentially advantageous channel characteristics. In the region around the arms and legs of the the rear passengers, useful for devices such as tablet PCs, between $15\,\mu\mathrm{W}$ and $45\,\mu\mathrm{W}$ can be received with a reduction of no more than $< 0.1\,\mathrm{dB}$ when located away from the legs under all passenger configurations. In the region around the passengers shoulders and neck, where devices such as IR headphones or hands free voice equipment might be employed, up to $40\,\mu\mathrm{W}$ of power can be received with only a $0.2\,\mathrm{dB}$ reduction under all passenger scenarios. The use of the front seat headrests for placement of video screens or computer monitors is also illustrated. Currently in a non-optimised configuration, between $3.8\,\mu\mathrm{W}$ and $4.2\,\mu\mathrm{W}$ is received and this power is reduced by less than $0.8\,\mathrm{dB}$ under all passenger scenarios considered. Finally all results are shown to have sufficient bandwidth and an acceptable maximum RMS delay spread for use in high speed OW communications. It is hoped that these results, now incorporating the presence of multiple passengers in multiple configurations, in conjunction with an earlier analysis on channel viability [5], [6] will enhance the appeal of employing OW in this application.

References

[1] F. Bai and B. Krishnamachari, "Exploiting the wisdom of the crowd: localized, distributed information-centric VANETs," *IEEE Commun. Mag.*, vol. 48, no. 5, pp. 138 –146, May 2010.

[2] K. Dar, M. Bakhouya, J. Gaber, M. Wack, and P. Lorenz, "Wireless communication technologies for ITS applications," *IEEE Commun. Mag.*, vol. 48, no. 5, pp. 156 –162, May 2010.

[3] R. J. Green, H. Joshi, M. D. Higgins, and M. S. Leeson, "Recent developments in indoor optical wireless systems," *IET Commun.*, vol. 2, no. 1, pp. 3–10, Jan 2008.

[4] R. J. Green, "Optical wireless with application in automotives," in *Proc. IEEE ICTON*, 2010, p. We.C3.2.

[5] M. D. Higgins, R. J. Green, and M. S. Leeson, "Channel viability of intra-vehicle optical wireless communications," in *Proc. IEEE GLOBECOM Workshops*, 2011, pp. 813 –817.

[6] M. D. Higgins, R. J. Green, and M. S. Leeson, "Optical wireless for intravehicle communications: A channel viability analysis," *IEEE Trans. Veh. Tech.*, vol. 61, no. 1, pp. 123 –129, Jan. 2012.

[7] B. T. Phong, "Illumination for computer generated pictures," *Commun. ACM*, vol. 18, no. 6, pp. 311–317, 1975.

[8] S. R. Perez, R. P. Jimenez, F. J. López-Hernández, O. B. G. Hernandez, and A. J. A. Alfonso, "Reflection model for calculation of the impulse response on IR-wireless indoor channels using ray-tracing algorithm," *Microwave. Opt. Technol. Lett.*, vol. 32, no. 4, pp. 296–300, 2002.

[9] C. R. Lomba, R. T. Valadas, and A. M. de Oliveira Duarte, "Experimental characterisation and modelling of the reflection of infrared signals on indoor surfaces," *IEE Proc. Optoelectron.*, vol. 145, pp. 191–197, 1998.

[10] M. D. Higgins, R. J. Green, and M. S. Leeson, "A genetic algorithm method for optical wireless channel control," *IEEE J. Lightwave Tech.*, vol. 27, no. 6, pp. 760–772, March 2009.

[11] M. D. Higgins, R. J. Green, M. S. Leeson, and E. L. Hines, "Multi-user indoor optical wireless communication system channel control using a genetic algorithm," *IET Commun.*, vol. 5, no. 7, pp. 937 –944, 2011.

[12] K. Dana, B. Van-Ginneken, S. Nayar, and J. Koenderink, "Reflectance and Texture of Real World Surfaces," *ACM Trans. on Graphics (TOG)*, vol. 18, no. 1, pp. 1–34, Jan 1999.

[13] M. Oren and S. Nayar, "Seeing Beyond Lambertś Law," in *European Conf. on Computer Vision (ECCV)*, vol. B, May 1994, pp. 269–280.

[14] D. Salomon, *Curves and Surfaces for Computer Graphics*, Springer, 2006.

[15] J. R. Barry, J. M. Kahn, W. J. Krause, E. A. Lee, and D. G. Messerschmitt, "Simulation of multipath impulse response for indoor wireless optical channels," *IEEE J. Sel. Areas Commun.*, vol. 11, no. 3, pp. 367–379, 1993.

[16] J. M. Kahn, W. J. Krause, and J. B. Carruthers, "Experimental characterization of non-directed indoor infrared channels," *IEEE Trans. Commun.*, vol. 43, no. 234, pp. 1613–1623, 1995.

[17] J. B. Carruthers and P. Kannan, "Iterative site-based modelling for wireless infrared channels," *IEEE Trans. Antennas Propag.*, vol. 50, no. 5, pp. 759–765, 2002.

[18] A. Lagae and P. Dutr, "An efficient ray-quadrilateral intersection test," *Journal of graphics, GPU, and game tools*, vol. 10, no. 4, pp. 23–32, 2005.

[19] A. S. Glassner, *An introduction to ray tracing*. London: Academic Press, 1989.

[20] C. R. Lomba, R. T. Valadas, and A. M. de Oliveira Duarte, "Efficient simulation of the impulse response of the indoor wireless optical channel," *Int. J. Commun. Syst.*, vol. 13, no. 7-8, pp. 537–549, 2000.

[21] M. R. Pakravan and M. Kavehrad, "Indoor wireless infrared channel characterization by measurements," *IEEE Trans. Veh. Technol.*, vol. 50, no. 4, pp. 1053–1073, July 2001.

[22] N. Navet, Y. Song, F. Simonot-Lion, and C. Wilwert, "Trends in automotive communication systems," *Proc. IEEE*, vol. 93, no. 6, pp. 1204 –1223, June 2005.

[23] T. Nolte, H. Hansson, and L. Bello, "Automotive communications-past, current and future," in *IEEE ETFA 2005*, vol. 1, 2005, pp. 8 pp. –992.

[24] A. Sangiovanni-Vincentelli and M. Di Natale, "Embedded system design for automotive applications," *Computer*, vol. 40, no. 10, pp. 42 –51, Oct. 2007.

[25] W. Tong, C. Tong, and Y. Liu, "A data engine for controller area network," in *Proc. Int. Conf. Computational Intelligence and Security*, 2007, pp. 1015 –1019.

[26] G. Leen and D. Heffernan, "TTCAN: a new time-triggered controller area network," *Microprocessors and Microsystems*, vol. 26, no. 2, pp. 77 – 94, 2002.

[27] T. Kibler, S. Poferl, G. Bock, H.-P. Huber, and E. Zeeb, "Optical data buses for automotive applications," *J. of Lightwave Tech.*, vol. 22, no. 9, pp. 2184 – 2199, Sept. 2004.

[28] F. Sethna, E. Stipidis, and F. Ali, "What lessons can controller area networks learn from flexray," in *IEEE VPPC*, 2006, pp. 1 –4.

[29] M. Ahmed, C. Saraydar, T. ElBatt, J. Yin, T. Talty, and M. Ames, "Intra-vehicular wireless networks," in *Proc. IEEE GLOBECOM Workshops*, 2007, pp. 1 –9.

[30] M. Weihs, "Design issues for multimedia streaming gateways," in *Proc. ICN/ICONS/MCL*, 2006, p. 101.

[31] G. Leen and D. Heffernan, "Vehicles without wires," *Computing Control Engineering Journal*, vol. 12, no. 5, pp. 205 –211, Oct. 2001.

[32] D. Porcino and W. Hirt, "Ultra-wideband radio technology: potential and challenges ahead," *IEEE Commun. Mag.*, vol. 41, no. 7, pp. 66 – 74, July 2003.

[33] N. Baker, "Zigbee and bluetooth strengths and weaknesses for industrial applications," *Computing Control Engineering Journal*, vol. 16, no. 2, pp. 20 –25, April-May 2005.

[34] British Standard, "BS EN 60825: Safety of Laser Products."

[35] J. R. Barry, *Wireless infrared communications*. Kluwer Academic, 1994.

Matthew D. Higgins received his MEng in Electronic and Communications Engineering and PhD in Engineering from the School of Engineering at the University of Warwick in 2005 and 2009 respectively. Remaining at the University of Warwick, he then progressed through several Research Fellow positions with leading defence and telecommunications companies before undertaking two years as a Senior Teaching Fellow. Dr. Higgins now holds the position of Assistant Professor where his major research interests are

the modelling of optical propagation characteristics in underwater, indoor and atmospheric conditions and how the channel can affect communications systems. Dr. Higgins is a Member of both the IEEE and IET.

Roger J. Green became Professor of Electronic Communication Systems at Warwick in September 1999, and was Head of the Division of Electrical and Electronic Engineering from August 2003 for five years. He has published around 270 papers in the field of optical communications, optoelectronics, video and imaging, and has several patents. Over 57 Ph.D. research students have worked successfully under his supervision. He now leads the Communications Systems Laboratory in the School of Engineering at Warwick. His current interests include signal processing, optical wireless and optical fibre communications. He holds a Higher Doctorate (DSc) in Photonic Communications, Systems and Devices, is a Fellow of the UK IET and a Fellow of the Institute of Physics. He is a Senior Member of the IEEE, and currently serves on two IEEE committees concerned with communications and signal processing, and is a member of the COST IC1101 European project OPTICWISE.

Mark S. Leeson received the degrees of BSc and BEng with First Class Honors in Electrical and Electronic Engineering from the University of Nottingham, UK, in 1986. He then obtained a PhD in Engineering from the University of Cambridge, UK, in 1990. From 1990 to 1992 he worked as a Network Analyst for National Westminster Bank in London. After holding academic posts in London and Manchester, in 2000 he joined the School of Engineering at Warwick, where he is now an Associate Professor (Reader) and leads the Communication Networks Laboratory. His major research interests are coding and modulation, nanoscale communications and evolutionary optimization. To date, Dr. Leeson has over 220 publications and has supervised 12 successful research students. He is a Senior Member of the IEEE, a Chartered Member of the UK Institute of Physics and a Fellow of the UK Higher Education Academy.